Blame-Free Motion Planning in Hybrid Traffic

by

Sanggu Park

A Thesis Presented in Partial Fulfillment
of the Requirements for the Degree
Master of Science

Approved May 2022 by the
Graduate Supervisory Committee:

Aviral Shrivastava, Chair
Yezhou Yang
Ruoyu Wang

ARIZONA STATE UNIVERSITY

August 2022

ABSTRACT

Recent advances in autonomous vehicle (AV) technologies have ensured that autonomous driving will soon be present in real-world traffic. Despite the potential of AVs, many studies have shown that traffic accidents in hybrid traffic environments (where both AVs and human-driven vehicles (HVs) are present) are inevitable because of the unpredictability of human-driven vehicles. Given that eliminating accidents is impossible, an achievable goal of designing AVs is to design them in a way so that they will not be blamed for any accident in which they are involved in. This work proposes BlaFT – a Blame-Free motion planning algorithm in hybrid Traffic. BlaFT is designed to be compatible with HVs and other AVs, and will not be blamed for accidents in a structured road environment. Also, it proves that no accidents will happen if all AVs are using the BlaFT motion planner and that when in hybrid traffic, the AV using BlaFT will be blame-free even if it is involved in a collision. The work instantiated scores of BlaFT and HV vehicles in an urban road scape loop in the 'Simulation of Urban MObility', ran the simulation for several hours, and observe that as the percentage of BlaFT vehicles increases, the traffic becomes safer. Adding BlaFT vehicles to HVs also increases the efficiency of traffic as a whole by up to 34%.

TABLE OF CONTENTS

INTRODUCTION

With recent advances in machine learning, sensor accuracy, and edge-computing, Autonomous Vehicles (AVs) are getting closer to becoming a reality. Improvements in safety, traffic efficiency, and accessibility are being touted as the main benefits of the technology. However, before reaching the often imagined world of all AVs, there is likely to be a long transition period where autonomous vehicles have to operate along-with human-driven vehicles. Ideally, humans would like to build AVs that can avoid all accidents. However, several studies have shown that it is not possible for an AV to avoid all accidents in a hybrid traffic where AVs and human-driven vehicles (HVs) co-exist [1]. To understand this, consider a simple example situation where an AV is traveling on a multi-lane street, and the vehicles surrounding the AV come closer and cause a crash (figure 1.1. Given that accidents are unavoidable, a recent paper [2] argued that it may be possible to design vehicles that are not blamed for any accident in which they are involved in. Building an AV that will not be blamed for an accident is clearly very valuable to AV manufacturers and operators as they will not have to suffer any liability. In March 2022, Mercedes announced that they will accept legal responsibility of their autonomous driving system [3] even though it is only Level 3 system.

As per the restatement of the US Law Second torts, 454: *injurers are liable for accident damages, if any of the two conditions are satisfied. First, of course, the injurer must have acted negligently – that is, he must have exercised less than "due care" (negligence), or secondly, the injurer's negligence must have caused the accident (causation).* Based on this [4] concludes that to avoid blame for an accident in which a vehicle is involved, it must prove that i) the vehicle did not cause the accident (causation), AND ii) they did their "due diligence" to avoid the accident (negligence).

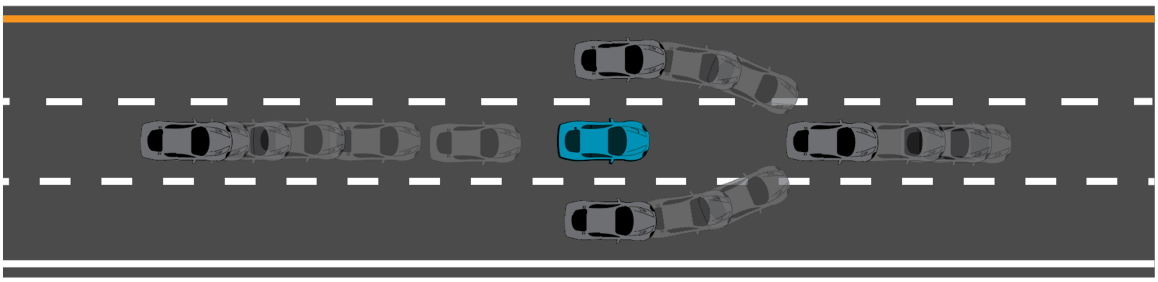

Figure 1.1: AV (blue car) cannot avoid all accidents. Other vehicles (grey cars) can crash into the AV. The best an AV can do is to not be blamed for any accident it is involved in.

This work codifies this blame definition into a motion planning algorithm and produce **BlaFT** – a **Bla**me-**F**ree motion planning algorithm for autonomous vehicles in hybrid **T**raffic. This paper makes the following contributions:

- The research proposes **BlaFT** – A '**Bla**me-**F**ree motion planner for hybrid **T**raffic, which will not be blamed for any accident in which it is involved in. This is achieved by ensuring that AV has the right-of-way during accident, **AND** the AV does it's best to avoid the accident.

- The research provides a safety proof that shows that in structured road environment where all traffic is composed of AVs running BlaFT, there will be no accidents.

- The research provides a blame proof that shows that in a hybrid environment, the vehicle running **BlaFT** will never be blamed for the accident.

Furthermore, to demonstrate the benefits of 'BlaFT' on safety and efficiency in hybrid traffic, the work implemented hybrid traffic simulation in an urban roadscape loop in the Simulated Urban Mobility (SUMO) traffic simulator [5]. In the simulation, the human-driven vehicles (HVs) are intentionally designed to drive in unsafe way to cause accidents. Adjusting the ratio of **BlaFT** to HVs from 0% to 100%, the work empirically proves i) As **BlaFT**-to-HV ratio increases, the number of collisions

linearly decrease, reaching no collisions when all the vehicles are **BlaFT** vehicles; and ii) Adding **BlaFT** vehicles increases the efficiency of the traffic by eliminating the chaotic behavior of HVs by up to 34% as compared to HV-only traffic.

RELATED WORK

As AVs are becoming more prevalent in traffic, issues of compatibility between AVs and HVs in hybrid traffic have been raised [6, 7]. [7] suggests that AVs need to predict the other vehicle's behaviors by estimating the externally measurable indicators (such as position, velocity, heading angle, etc.), regardless of whether the other vehicle is an HV or AV. On the other side, since HVs cannot distinguish if the other one is AV or HV, AV's driving should be indistinguishable from HVs to prevent disturbance to current traffic safety.

To address the AV compatibility while satisfying the safe condition, [2] propose RSS rules which make AVs to maintain longitudinal and lateral safe distances and decide proper Right-Of-Way (ROW) for the merging case. [2] proves that RSS guarantees the longitudinal safety in case vehicles are in same lane and they maintain the longitudinal safe distance from the front one. The remaining rules are also based on the inter-vehicular distances. However, [2]'s approach and proofs ignored finite lane width, and that can cause their AV algorithm to be blamed for lateral accidents. Furthermore, they use distance to the merge point as the metric to decide right-of-way, which is not necessarily compatible with human driving. This makes their AV incompatible with human-driven vehicles.

Meanwhile, to prove lateral safety of autonomous driving algorithm, [1] provides formal expressions for full autonomous driving in multi-lane traffic. Distinguishing the driver's behaviors to be lane-following (LF) and lane-changing (LC), [1]'s algorithm proves that lateral safety between LF and LC is possible whenever LC maintains the reserved space in target lane to be empty. However, it still admits the lateral safety is only possible when both LF and LC participating in LC process are equipped with the same motion planner and they explicitly understand the other's driving (or only for

AV-only traffic). In other words, it is impossible for AVs in hybrid traffic to be safe, because of unidentifiable ROW decisions among drivers who use the heterogeneous motion planning methods.

To understand the other driver's vague intentions and make AVs to adapt to them, recent studies introduced game-theoretic methods [8, 9]. By translating the driving process in structured road into a Stackelberg (or leader-follower) model, they propose reward functions which score each of the human's possible decisions in a human-like way and choose the most optimal one. However, these game-theoretic predictions cannot provide any safety or blame guarantees due their inherently probabilistic nature.

Several collision avoidance and mitigation (CAM) algorithms are proposed to guarantee more 'safer' situation, however, they cannot guarantee collision-free traffic due to the limitations suggested previously. Not only that, the safety concepts are differently defined for each individual research so that the collision decision point (when or where to estimate the possible collision) differs by each other or even unclear [10, 11, 12]. Because the accident in hybrid traffic is always possible, the best AV (or manufacturer) can do is to avoid blame, when the AV is involved in the accident [13]. To be free from blame, the current law requires the victim to prove that there was no 'negligence' AND 'causation' for itself [4].

DEFINITIONS

In this section, we discuss definitions of safety envelopes, safe situation, and blame definitions that are used to design BlaFT.

3.1 Stopping Distances

We define 2 levels of braking for a vehicle. First is $a_{dec,max}$ – which is the maximum braking of the vehicle, and second is the $a_{dec,res}$ – which is the responsive braking that the vehicle seeks to apply, if it senses danger. Response braking is a target braking threshold that human vehicles in a hybrid environment expect other vehicles to typically apply. We define stopping distance of the vehicle with respect to the $a_{dec,max}$ as d_c using equation 3.1 and $a_{dec,res}$ as d_r using equation 3.2. These equations take into into consideration the sense-to-actuation time (ρ). We assume the worst case, that during the (ρ time) the vehicle is accelerating at the maximum rate. Thus:

$$d_c = v \cdot \rho + \frac{1}{2} a_{acc,max} \cdot \rho^2 + \frac{(v + \rho \cdot a_{acc,max})^2}{2a_{dec,max}} \tag{3.1}$$

$$d_r = v \cdot \rho + \frac{1}{2} a_{acc,max} \cdot \rho^2 + \frac{(v + \rho \cdot a_{acc,max})^2}{2a_{dec,res}} \tag{3.2}$$

Crash and Response Envelope: Corresponding to these two braking and two stopping distances, we define two trajectory envelopes for a vehicle. The *Crash Envelope (CE)* – of length d_c, and the *Response Envelope (RE)* – of length d_r, and the width equal to the width of the vehicle w. Using the lane-based coordinate system from [2], we define CE and RE as:

$$CE = \{t(Y) + \alpha \cdot w(Y) \cdot t^{\perp}(Y) | Y \in [Y_{tail}, Y_{head} + d_c], \alpha \in [\pm 1/2]\} \tag{3.3}$$

$$RE = \{t(Y) + \alpha \cdot w(Y) \cdot t^{\perp}(Y) | Y \in [Y_{tail}, Y_{head} + d_r], \alpha \in [\pm 1/2]\} \tag{3.4}$$

where the Y-axis is the curve of the center line of the trajectory of the vehicle, starting from Y_{tail} to Y_{head}. $t(Y)$ is the trajectory of the vehicle in the direction of the center line of the lane, w is the width of the vehicle. The parameters $\alpha \in [\pm 1/2]$ allow all the points around the trajectory-line within the width of the vehicle to be included in the envelope.

One key idea in the driving algorithm of the AV is that at each time-step (of ρ time), if the AV senses another vehicle's estimated trajectory to overlap with the RE, then the AV will update its motion plan to avoid the overlap. If another vehicle's estimated trajectory overlaps with the CE of the AV, then the accident may be unavoidable.

Figure 3.1: Vehicles are in $safe$ state, if their REs (green shade) do not overlap (left) or if the REs overlap, but CEs do not overlap (right). This is because both vehicles can avoid the accident by proper braking.

3.2 Safe and Crash States

From the perspective of an AV, we can define it's state with respect to another vehicle at a moment in time as a *crash state*, *safe state* or *blame-free state*. An AV is in a *crash state* with another vehicle, if the (Crash Envelope) CE of the other vehicle overlaps with the CE of the AV. This is because AV may not be able to avoid the accident. If the vehicles are not in a *crash state*, we define them to be in a *safe state*. This is because the AV can slow down to avoid the accident. Thus:

$$crash \equiv \forall c : c \neq ego \wedge \langle CE_c \cap CE_{ego} \rangle \tag{3.5}$$

$$safe \equiv \neg crash \tag{3.6}$$

Figure 3.2: Two vehicles are in a *crash* state, if the CEs of two vehicles overlap. The accident may be un-avoidable. In the left figure the blue vehicle has the ROW, while in the right figure the red one has ROW.

3.3 Blame-free State

To determine whether AV is to be blamed or not, we follow [4]'s two blame conditions, causation and negligence. As per [4], a vehicle will be blamed for an accident if it caused the accident (causation) **OR** it could have avoided the accident (negligence). Thus:

$$blame\text{-}free \equiv safe \vee \big(crash \wedge \neg causation \wedge \neg negligent\big) \tag{3.7}$$

Causation is determined by Right-of-Way (ROW). Thus, we define that the vehicle without ROW causes the accident. ROW is determined from the structured road rules, such a yield sign indicating that the ego would not have the right of way when merging.

$$causation_{ego} \equiv \neg ROW_{ego} \tag{3.8}$$

We define a the collision to be not negligent whenever the '*crash*' condition appears with no prior warning. This means the **RE** area of the other vehicle did not pass through AV's **RE** in at least the previous time step. Therefore the AV never had a chance to react the to potential collision and avoid it.

$$\begin{aligned} negligent_{ego} \equiv \forall c : c \neq ego \\ \wedge \Big\langle \big(RE_{ego} \cap \neg CE_{ego}\big) \cap RE_c \Big\rangle \end{aligned} \tag{3.9}$$

By substituting equations 3.8 and 3.9 into equation 3.7, we derive an equation 3.10. It concludes that an AV is $blame\text{-}free$ whenever it is $safe$ or proves it had the right-of-way against the other car 'c'.

$$\begin{aligned} blame\text{-}free \equiv safe \wedge \Big(& crash \wedge ROW_{ego} \\ & \wedge \neg \big\langle \big(RE_{ego} \cap \neg CE_{ego} \big) \cap RE_c \big\rangle \Big) \\ & \leftrightarrow safe \wedge \big(crash \wedge ROW_{ego} \big) \end{aligned} \tag{3.10}$$

ALGORITHM

Algorithm 1 outlines our **BlaFT** – A '**Bla**me-**f**ree' motion planning algorithm which works in hybrid **T**raffic. **BlaFT** consists of four parts: behavior decision, conservative sensing, collision detection, and the collision avoidance and mitigation (CAM). **BlaFT** is a motion planning algorithm and runs at a high frequency. A relatively infrequent routing algorithm runs concurrently on the top of this motion planning algorithm, and provides the context for the motion planning algorithm – specifically, it provides it with the set of waypoints (WP) to follow towards the destination.

Algorithm 1 BlaFT Driving

1: **while** not at destination **do**

2: $BH = decide\_behavior(WP, \boldsymbol{z}_{ego}, G, d_{blink})$

3: $\hat{\boldsymbol{z}}_c = conservative\_sensing(\boldsymbol{z}_c)$

4: $CA = detect\_collision(BH, \hat{\boldsymbol{z}}_c)$

5: $W', a' = CAM(WP, G, \hat{\boldsymbol{z}}_c, collision)$

6: $\boldsymbol{z}_{ego} \leftarrow motion\_control(WP', a')$

7: $WP \leftarrow WP'$

4.1 Behavior Decision

As the first step of the algorithm, **BlaFT** decides whether it plans to continue on current the lane (Lane Following or LF), or it plans to change it's lane (Lane Changing or LC). An AV may want to change lane due to variety of reasons such as to follow it's route to the destination, to optimize the time of travel / fuel efficiency, or even to avoid accidents.

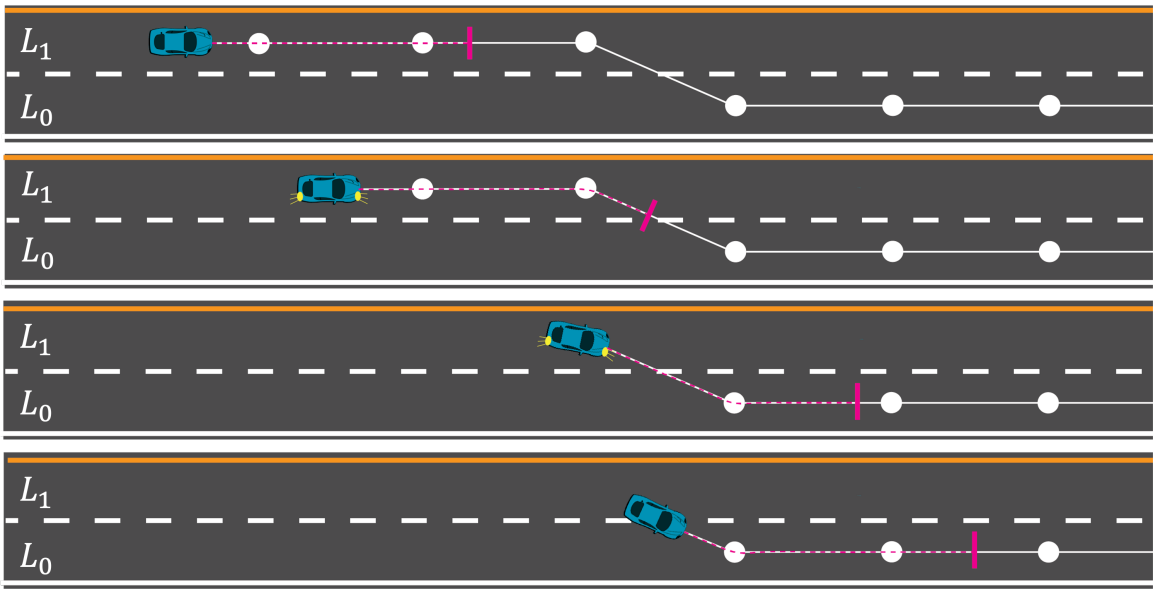

Figure 4.1: Demonstration of behavior decision. Ego AV (blue car) draws BL (pink line) which is 'd_{blink}' distant alongside the planned trajectory (white line). If *ego* and BL overlap with the lane L_1 only, then AV is in LF mode (top). However, if BL starts to overlap with L_0 but *ego* does not, AV is in LC mode (middle). After entering the target lane, then *ego* overlaps with L_0 and recovers back to the LF mode (bottom).

$$BL = \{t(Y) + \alpha \cdot w_{ego} \cdot t^{\perp}(Y) | Y = Y_0 + d_{blink}, \alpha \in [\pm 1/2]\} \tag{4.1}$$

$$behavior = \begin{cases} LC, & \exists L_i \in L : \langle BL_{ego} \cap L_i \rangle \wedge \neg \langle ego \cap L_i \rangle \\ LF, & otherwise \end{cases} \tag{4.2}$$

4.2 Conservative Sensing

This step uses the sensed data that the AV has collected to project the worst case future trajectory of the other vehicles on the road considering the error margin of the sensor(s). The sensing information consists of the location (x_c, y_c), the heading angle θ_c, and the velocity v_c of each of the vehicles it observes in it's sensing range.

$$\boldsymbol{z}_c = \begin{pmatrix} x_c & y_c & \theta_c & v_c \end{pmatrix}^T \tag{4.3}$$

To calculate other vehicles' near-future trajectories, **BlaFT** uses the Constant Turn Rate and Velocity (CTRV) model [14]. In CTRV, the differentials of turning

angle (θ) and of velocity (v) are assumed to be constants 'ω' and '0', respectively where 'ω' is the maximum steering angular velocity. Based on the constants, **BlaFT** predicts other vehicle's near-future information ($\boldsymbol{z}'_c$) as an equation 4.4.

$$\boldsymbol{z}'_c = \begin{pmatrix} x'_c \\ y'_c \\ \theta'_c \\ v'_c \end{pmatrix} = \begin{pmatrix} x_c + \frac{v}{\omega} \cdot \sin\left(\theta_c + \omega\Delta t\right) - \frac{v}{\omega} \cdot \sin\theta_c \\ y_c - \frac{v}{\omega} \cdot \cos\left(\theta_c + \omega\Delta t\right) + \frac{v}{\omega} \cdot \sin\theta_c \\ \theta_c + \omega\Delta t \\ v_c \end{pmatrix} \tag{4.4}$$

Lastly, **BlaFT** uses the worst-case sensing information which is within the the range of z_c's over the error margins of the values. The worst-case sensing information ($\hat{\boldsymbol{z}}_c$) is set to minimize the distance between the vehicle c's position and the ego's vehicle's position at the time of '$t + \Delta t$' (equation 4.5, 4.6). Then, **BlaFT** is able to draw the worst case trajectory of the of all the other vehicles in the sensing range of the AV.

$$\hat{\boldsymbol{z}}_c = \begin{pmatrix} \hat{x_c} \\ \hat{y_c} \\ \hat{\theta_c} \\ \hat{v_c} \end{pmatrix} = \underset{\hat{\boldsymbol{z}}_c}{\operatorname{argmin}} \left([D'_{c,ego} | \hat{\boldsymbol{z}}_c \in [\boldsymbol{z}_c \pm \epsilon_{\boldsymbol{z}}] \right) \tag{4.5}$$

$$D'_{c,ego} = \sqrt{(\hat{x}'_c - x'_{ego})^2 + (\hat{y}'_c - y'_{ego})^2} \tag{4.6}$$

4.3 Collision Detection

Once **BlaFT** derives the worst-case trajectories of the other vehicles, it determines the potential collision area. **BlaFT** draws the envelopes of itself and of the sensed vehicles, and searches for the overlap between them. Then, the union of the overlapped areas is considered to be the potential collision area. And the way **BlaFT** draws the

envelopes depends on whether it is in LF or LC mode. The process is described in algorithm 2 and Fig. 4.2, 4.3.

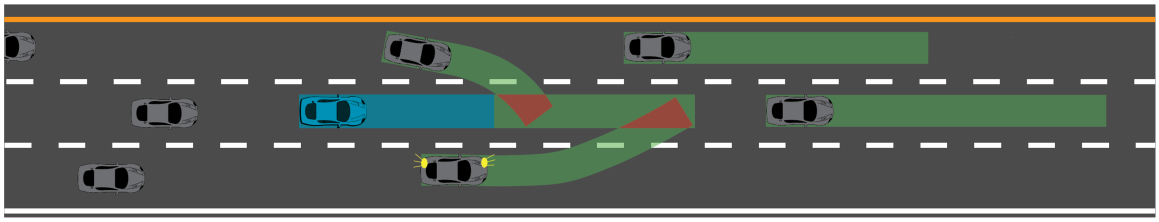

Figure 4.2: Collision detection in lane-following mode. Ego AV (blue car) draws CE_{ego} (blue shade), RE_{ego} (green shade), and the worst case $\hat{RE}_c$ of other vehicle c (grey car). If ego AV detects the overlap(s) between them (red shades), the union of the overlaps becomes the collision area.

First, if AV is in LF mode, the default collision area (CA) is set to be an empty set and **BlaFT** draws 'RE_{ego}' (line 1-2). Then, **BlaFT** creates the worst-case response envelopes '$\hat{RE}_c$' for all other vehicles $c \in C$, which are longitudinally in front (line 3-6). Now, CA is the union of the overlaps between RE_{ego} and $\hat{RE}_c$ (line 7).

Algorithm 2 Collision Detection

Input: WP, BH, $\hat{\boldsymbol{z}}_c$, $\boldsymbol{z}_{ego}$

Output: CA

1: $CA = \emptyset$

2: $RE_{ego} = create\_RE(WP, \boldsymbol{z}_{ego})$

3: **for all** $c \in C$ **do**

4: **if** $Y_c > Y_{ego}$ **then**

5: $\hat{RE}_c = create\_RE(\hat{\boldsymbol{z}}_c)$

6: $CA = CA \cup \left(RE_{ego} \cap \hat{RE}_c\right)$

7: **if** $BH = LC$ **then**

8: $LE_{ego} = create\_LE(WP, \boldsymbol{z}_{ego}, t_{blink})$

9: **for all** $c \in C$ **do**

10: **if** $L_c \neq L_{ego} \wedge Y_c < Y_{ego}$ **then**

11: $\hat{RE}_c = create\_RE(\hat{\boldsymbol{z}}_c, W_L(Y_c), t_{enter})$

12: **if** $LE_{ego} \cap \hat{RE}_c \neq \emptyset$ **then**

13: $CA = CA \cup \left(RE_{ego} \cap LE_{ego}\right)$

14: **break**

15: **return** CA

However, if **BlaFT** is in LC mode, **BlaFT** additionally draws a Lane-Change Envelope (LE) (line 7-8). LE is essentially the RE in the target lane that the ego vehicle will draw at the moment it starts to enter the new lane (equation 4.7). And that is the reason why the range of Y is from Y^{lc} to $Y^{lc} + d_r$, where Y^{lc} is the Y-axis position of the vehicle when it changes lane.

$$LE_{ego} = \{t(Y) + \alpha \cdot w(Y) \cdot t^{\perp}(Y) | Y \in [Y^{lc}, Y^{lc} + d_r], \alpha \in [\pm 1/2]\} \tag{4.7}$$

The collision detection in LC mode is depicted in Fig. 4.3. To detect the potential

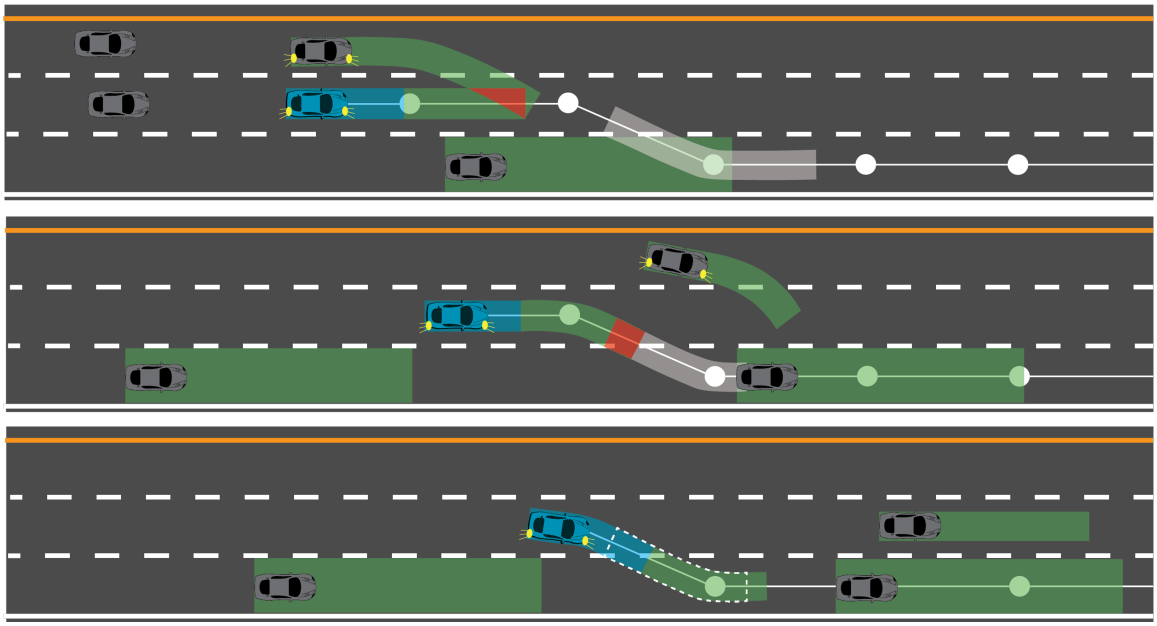

Figure 4.3: Collision detection in lane-changing mode. While conducting the collision detection same as LF (top), ego AV additionally draws LE_{ego} on the target lane (white shade). If ego AV detects the overlap between LE_{ego} and $\hat{RE}_c$, $RE_{ego} \cap LE_{ego}$ is considered to be the collision (top, middle). Otherwise, if no overlap exists (bottom), AV neglects the area of LE_{ego} (empty white box).

collision in the target lane with the LE_{ego}, **BlaFT** draws the Response Envelopes ($\hat{RE}_c$) of all the other surrounding vehicles (except the rear vehicles in the same lane) assuming that their response time to be $\rho_c + t_{enter}$ (line 10-12). This essentially has the effect of elongating the $\hat{RE}_c$ to cover the area that the other vehicle could be in, even if it did not notice the ego vehicle while ego vehicle was entering, and the vehicle accelerated to it's maximum. Furthermore, in order to prevent the ego vehicle to even partially enter the target lane if it is not safe, **BlaFT** widens the $\hat{RE}_c$ of the other vehicles in the target lane to cover the whole width of the target lane ($W_L(Y)$), instead of the vehicle width ($W_c(Y)$) (line 12). Once the envelopes are drawn, **BlaFT** searches for the overlap between LE_{ego} and $\hat{RE}_c$. If there is an overlap, then the overlap between RE_{ego} and LE_{ego} becomes the CA (line 13-14). If there is no overlap, then LE_{ego} becomes an empty set and there is no CA in the

target lane area.

4.4 Collision Avoidance and Mitigation

When **BlaFT** detects a potential collision area, it tries to come up with a pair of alternative trajectory (WP') and acceleration rate (a') so as to avoid the collision. If the collision area is unavoidable, **BlaFT** applies maximum braking to minimize the impact of collision. The overall process is outlined in algorithm 3.

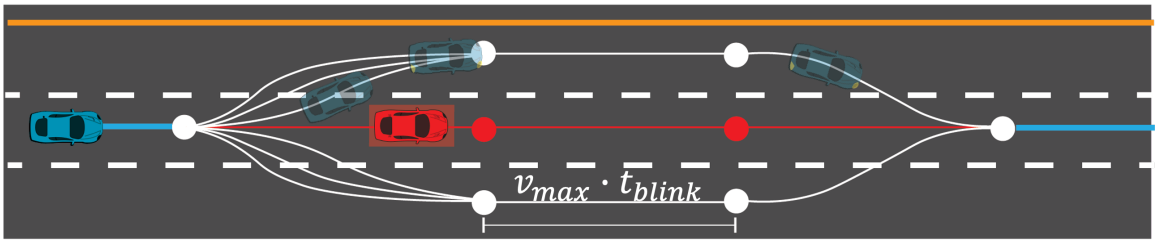

Figure 4.4: Re-routing step. Ego AV (blue) extracts the alternative trajectories after removing the nodes (red circle) in the road graph which is close to the collision area (red rectangle). The extracted trajectories enable the ego AV to be spatially disjoint against the the collision area.

To start with, the default response is set to be a pair of current trajectory and maximum braking rate (line 1). If ego AV detected no collision area (line 2), it tries to find out the most proper acceleration rate while maintaining the current trajectory (line 3). In contrast, if the collision area is detected, it updates the road graph by removing the nodes and edges (line 4-5). The removed ones are close to the collision area, as shown in Fig. 4.4. To enable AV to take sufficient time to take over the collision area, the length of removed nodes and edges should be longer than '$d_{blink} = v_{max} \cdot t_{blink}$'. Then, it finds out all possible trajectories to reach the destination (line 6).

Subsequently, **BlaFT** applies all possible acceleration rates $a \in [a_{acc,max}, -a_{dec,max}]$ (searching from $a_{acc,max}$ to pursue the fastest velocity) to find out the collision area (CA') by the response alongside each alternative trajectory (WP'). Using the future

Algorithm 3 Collision Avoidance and Mitigation

Input: CA, $\boldsymbol{z}_{ego}$, $\hat{\boldsymbol{z}}_c$, WP, M

Output: $response$

1: $response = (WP, -a_{dec,max})$
2: **if** $CA = \emptyset$ **then**
3: $\quad WP' = WP$
4: **else if** $CA \neq \emptyset$ **then**
5: $\quad M' = remove\_colliding\_nodes(M, CA, d_{blink})$
6: $\quad WP' = reroute\_trajectory(\boldsymbol{z}_{ego}, dst, M')$
7: **for all** WP' **do**
8: $\quad$ **for all** $a' \in [a_{acc,max}, -a_{dec,max}]$ **do**
9: $\quad\quad \boldsymbol{z}'_{ego} = update\_velocity(\boldsymbol{z}_{ego}, a')$
10: $\quad\quad$ **if** $(v'_{ego} \geq v_{max}) \vee (a'_{lat} \geq a_{lat,max})$ **then**
11: $\quad\quad\quad$ **continue**
12: $\quad\quad BH' = decide\_behavior(WP', \boldsymbol{z}'_{ego}, G)$
13: $\quad\quad CA' = detect\_collision(\boldsymbol{z}'_{ego}, \hat{\boldsymbol{z}}_c, WP', BH')$
14: $\quad\quad$ **if** $CA' = \emptyset$ **then**
15: $\quad\quad\quad response = (WP', a')$
16: $\quad\quad\quad$ **return** $response$
17: **return** $response$

velocity ($v'_{ego} = v_{ego} + a \cdot \Delta t$), **BlaFT** checks if the future velocity and the centrifugal acceleration (a'_{lat}) exceeds the maximum constrained values (line 7-9). The centrifugal acceleration is calculated by using the maximum curvature of the trajectory (κ) and the future velocity (v') as an equation 4.8. If it violates the condition, then it goes to the next iteration (line 10-11).

$$a'_{lat} = \kappa \cdot v'^2 < a_{lat,max} \tag{4.8}$$

If the condition is met, **BlaFT** predicts its future behavior(BH') and future collision area (CA') (line 12-13). And it uses the same methods proposed in previous sections. If no collision area is detected, then **BlaFT** returns a pair of the trajectory and the acceleration rate as a response (line 14-16). Otherwise, it continues the searching.

Despite the searching, if **BlaFT** could not return the safe response, then it means there is no option for the collision avoidance. In this case, **BlaFT** returns the default response which consists of the current trajectory and the maximum deceleration rate '$a_{dec,max}$' to mitigate the damage (line 17).

PROOFS

In this section, we first prove that in a situation where all vehicles are known to be running **BlaFT**, there will not be any collisions (safety proof). Then, we also prove that in a hybrid traffic scenario a vehicle driving with **BlaFT** will not be blamed for any accident that it is involved in (blame proof). And the proofs are done by following the collision scenarios that AV might face. As depicted in a Fig. 1.1, we classify the scenarios into three: collision from the different lane(s), collision from a rear vehicle in the same lane, and collision with a vehicle in front in the same lane.

5.1 Safety Proof

Theorem 1. *If all vehicles on a structured road are driven by* ***BlaFT****, and they start from a* ***safe*** *state, then there will be no accident.*

Proof. We will prove this by mathematical induction on the time moments defined in multiples of ρ (the response time of *ego* vehicle). We will show that at any timestep k, the Collision Envelope of the *ego* vehicle CE_{ego} does not overlap with the CE_c of any other vehicle c. In fact:

$$\forall c : c \neq ego \wedge \neg\langle CE_c \cap CE_{ego}\rangle \tag{5.1}$$

Base Case ($t = 0$): We assume that the base case is true by the assumption in the theorem – that we start from a blame-free state. This implies that the CE_{ego} does not overlap with the CE_c of other vehicle 'c'.

Inductive Hypothesis ($t = k$): At some time step $t = k$, we assume the Collision Envelope of the '*ego*' vehicle CE_{ego} does not overlap with the the one of any other vehicle 'c' CE_c at time step k, i.e.,

$$\forall k \geq 0, \forall c : c \neq ego \wedge \neg\langle CE^{k}_{ego} \wedge CE^{k}_{c} \rangle \tag{5.2}$$

Inductive Step ($t = k + 1$): Now, we prove that CE^{k+1}_{ego} does not overlap with CE^{k+1}_{c} of any other vehicle c. We divide the proof by the behavior modes – i.e., whether the ego vehicle is in the lane following (LF) mode, or in the lane changing (LC) mode.

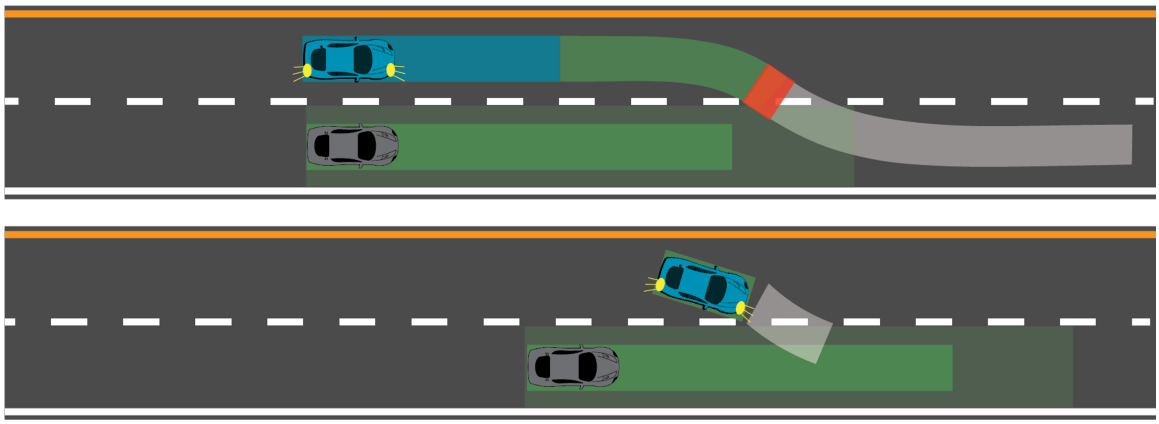

Figure 5.1: BlaFT (blue car) in LC-mode. If LE (white shade) overlaps with the other(grey car)'s estimated RE (shallow green shade), it does not overcome the LE. Due to this, the **BlaFT** in LC-mode does not allow the REs (thick green shades) to overlap.

To begin with, **BlaFT** in LC-mode does not allow the overlap between its LE and RE, whenever its LE overlaps with other vehicle's estimated RE (Fig. 5.1). And **BlaFT** does not enter the target lane until the overlap disappears. This prevents the overlap between the RE of ego vehicle and real RE of the other vehicle in the target lane. Thus, the lane-changing process satisfies equation 5.3.

$$\begin{aligned} &\forall c : c \neq ego \wedge \neg\langle RE^{k+1}_{ego} \cap LE^{k+1}_{ego} \rangle \\ &\rightarrow \forall c : c \neq ego \wedge \neg\langle RE^{k+1}_{ego} \cap RE^{k+1}_{c} \rangle \\ &\rightarrow \forall c : c \neq ego \wedge \neg\langle CE^{k+1}_{ego} \cap CE^{k+1}_{c} \rangle \\ &\leftrightarrow safe_{k+1} \end{aligned} \tag{5.3}$$

However, if **BlaFT** is in LF-mode in **BlaFT**-only traffic, all possible opponents can be in three categories: opponent from the adjacent lane(s), opponent from be-

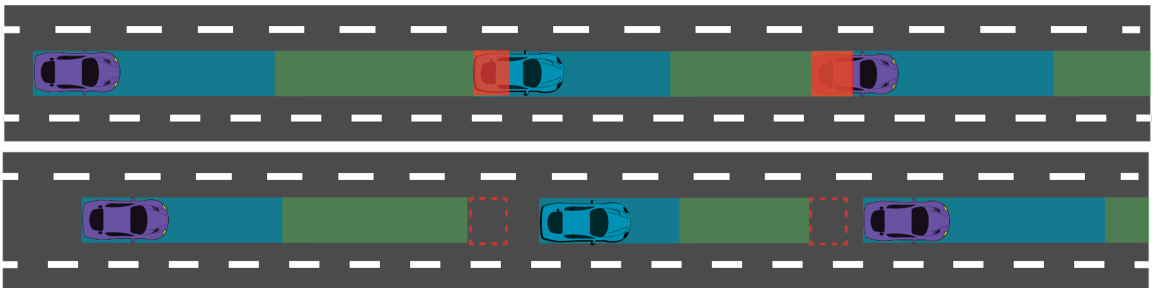

Figure 5.2: LF-mode AVs in **BlaFT**-only traffic. As collision areas are detected within $RE \cap \neg CE$ (red shades, upper), AVs are able to avoid them by braking (dashed boxes, lower).

hind, and from front. First, if one or more opponents come from the adjacent lanes, following the previous discussion, they do not allow the RE overlap. Second, the last remaining scenarios are the opponents are in the same lane as depicted in a Fig. 5.2. In this case, **BlaFT** is able to avoid the RE overlap with the front car by maintaining the enough distance.

$$\begin{aligned} &\forall c : c \neq ego \wedge \left\langle \left(RE_{ego}^{k+1} \cap \neg CE_{ego}^{k+1} \right) \cap RE_{c}^{k+1} \right\rangle \\ &\leftrightarrow \forall c : c \neq ego \wedge \neg \left\langle RE_{ego}^{k+1} \cap \hat{RE}_{c}^{k+1} \right\rangle \\ &\rightarrow \forall c : c \neq ego \wedge \neg \left\langle CE_{ego}^{k+1} \cap CE_{c}^{k+1} \right\rangle \\ &\leftrightarrow safe_{k+1} \end{aligned} \tag{5.4}$$

As a consequence of the induction, **BlaFT** satisfies '$safe$' state at every time step in **BlaFT**-only traffic.

□

Lemma 1. *If a vehicle suddenly appears in '$RE_{ego} \cap \neg CE_{ego}$' of a **BlaFT**, then **BlaFT** will be able to avoid crashing with it.*

Proof. The maximum length of the AV's overlapped area of RE('l_o') is less than the crash distance ('d_c'). Thus, if the collision area was outside the CE at '$t = k$', then ego vehicle is possible to avoid the accident by braking between 0 to maximum at '$t = k + 1$'.

$$0 \leq l_o = v \cdot \rho + \frac{1}{2} a_{acc,max} \cdot \rho^2 < d_c \tag{5.5}$$

□

5.2 Blame Proof

Theorem 2. *If **BlaFT** starts the driving from a **blame-free** state, then **BlaFT** will always maintain **blame-free** state.*

Proof. We will show that at any time k, *ego* vehicle is in $safe$ state or $crash \wedge ROW_{ego}$ state. In fact:

$$\forall c : c \neq ego \wedge safe \vee \big(crash \wedge ROW_{ego}\big) \tag{5.6}$$

Base Case ($t = 0$): We assume that the base case is true by the assumption in the theorem – that we start from a **blame-free** state. This implies that the ego AV is in the state either $safe$ or $crash \wedge ROW_{ego}$.

Inductive Hypothesis ($t = k$): At some time step $t = k$, we assume CE_{ego} does not overlap with CE_c or CE_{ego} overlaps with CE_c while *ego* possesses the right-of-way 'ROW_{ego}.' Thus:

$$\begin{aligned} &\forall k \geq 0, \forall c : c \neq ego \wedge \neg\big\langle CE^k_{ego} \wedge CE^k_c \big\rangle \\ &\vee \Big(\big\langle CE^k_{ego} \wedge CE^k_c \big\rangle \wedge ROW^k_{ego}\Big) \end{aligned} \tag{5.7}$$

Inductive Step ($t = k + 1$): Now, we prove the equation 5.7 at the time step $t = k+1$. We divide the proof by the modes of **BlaFT** – i.e., whether the ego vehicle is in the lane following (LF) mode, or in the lane changing (LC) mode.

First, same as the safety proof, **BlaFT** in LC-mode satisfies the state '$safe_{k+1}$.' When **BlaFT** is in LF-mode, there are three possible cases that its RE overlap: from the front or behind in the same lane, or from the adjacent lanes (Fig. 5.3). If **BlaFT**'s

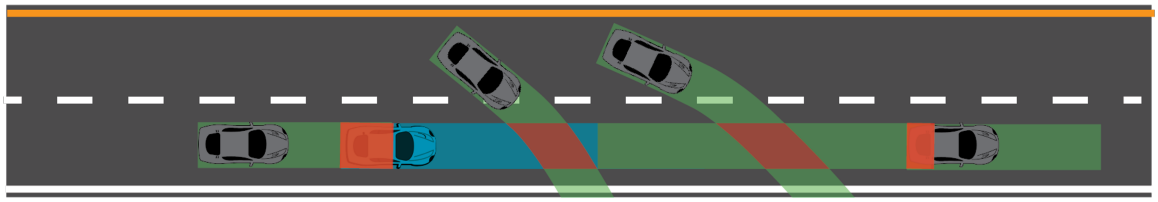

Figure 5.3: BlaFT (blue car) is in LF-mode in the hybrid traffic. It is safe from the front car (the rightmost red rectangle) by lemma 1. When it comes to the other vehicles from adjacent lane and the behind (the remaining red ones), **BlaFT** has the right-of-way. For this reason, if the accident came from the adjacent lane(s) or behind, **BlaFT** remains *blame-free*.

$RE_{ego} \cap \neg CE_{ego}$ overlaps with either the front one or the one from the adjacent lane(s), **BlaFT** is $safe_{k+1}$ by the Lemma 1. However, in the state $CE_{ego} \cap RE_c$ from behind or adjacent lane(s), **BlaFT** always has a right-of-way (ROW_{ego}). And all these facts are summarized in an equation 5.8. Following the equation, **BlaFT** in LF-mode is ***blame-free*** at every time step.

$$\begin{aligned} &\forall c : c \neq ego \wedge safe_{k+1} \vee \left(\langle CE_{ego} \cap RE_c \rangle \wedge ROW_{ego}\right) \\ &\leftrightarrow \forall c : c \neq ego \wedge safe_{k+1} \vee \left(crash_{k+1} \wedge ROW_{ego}\right) \\ &\leftrightarrow blame\text{-}free_{k+1} \end{aligned} \tag{5.8}$$

As a consequence of the induction, **BlaFT** satisfies '$blame\text{-}free_{k+1}$' state at every time step in hybrid traffic. □

In this section, we empirically evaluate how **BlaFT** affects real-scale traffic in terms of 'safety' and 'efficiency.' To do this, we have implemented **BlaFT** within SUMO simulator. We created a road environment that is conducive to infinite driving, shown in Fig. 6.1. And every vehicle in the simulation followed the naturalistic driving parameters [15]. The parameters are shown in a table 6.1. As shown in the table, AV assumes the other vehicle's '$a_{res,dec}$', '$a_{max,acc}$', and 'ρ' to be the worst-case ones during the driving, only to be safe from the misunderstanding of vehicular specifications. Plus, we set that AV's $a_{res,dec}$ vary in the range $2.0 \sim 7.0 m/s^2$ for each experiment, since AV can freely choose the deceleration rate which is below the maximum deceleration rate as $a_{res,dec}$. Furthermore, we have modified the HV's velocity to follow a normal distribution that averaged the maximum allowed velocity such that they occasionally make mistakes and cause a collision.

	$a_{res,dec}$ $[m/s^2]$	$a_{max,acc}$ $[m/s^2]$	ρ $[s]$	$a_{max,dec}$ $[m/s^2]$	$l \times w$ $[m \times m]$
AV	2.0˜7.0	1.8	0.1	7.0	5.0 × 1.8
HV	3.6	(4.1)	0.2		
(worst-case)	(4.6)		(0.5)		

Table 6.1: Naturalistic driving parameters in perspective of AVs. **BlaFT** predicts other vehicle's parameters to be the worst-case ones.

Then, we perform a simulation with a set ratio of HVs to AVs that are running **BlaFT** (e.g., 0:30, 5:25, etc.). Our simulation takes 30 vehicles, and we set the maximum velocity to either $12m/s$ or $25m/s$ to assume the typical city and highway driving for each. At $12m/s$, 30 vehicles in the environment can be translated into

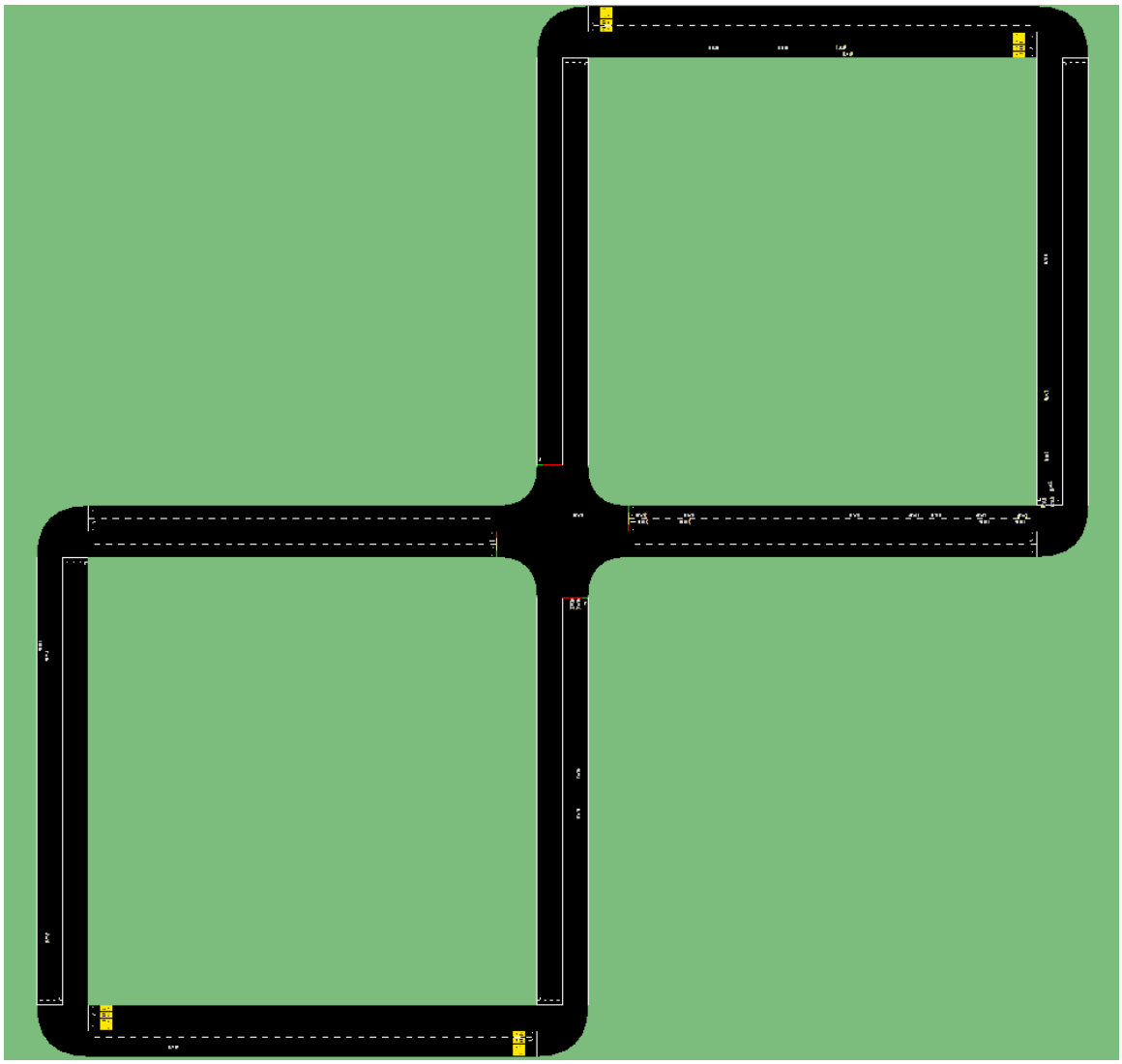

Figure 6.1: Road environment setup for the simulation. Two loops around the traffic light intersection consist of four lanes. The lane width is $3.2m$, and the length of each loop is $1km$.

throughput of approximately 400 $vehicles/lane \cdot hour$, and at $25m/s$ the throughput is approximately 800 $vehicles/lane \cdot hour$. Furthermore, to check the average results, experiments of 30-minute duration are done for 10 times for each data point. To check the safety and efficiency, we recorded two statistics using the existing analysis tools in SUMO, which are the number of collisions, and the delayed time of each vehicle.

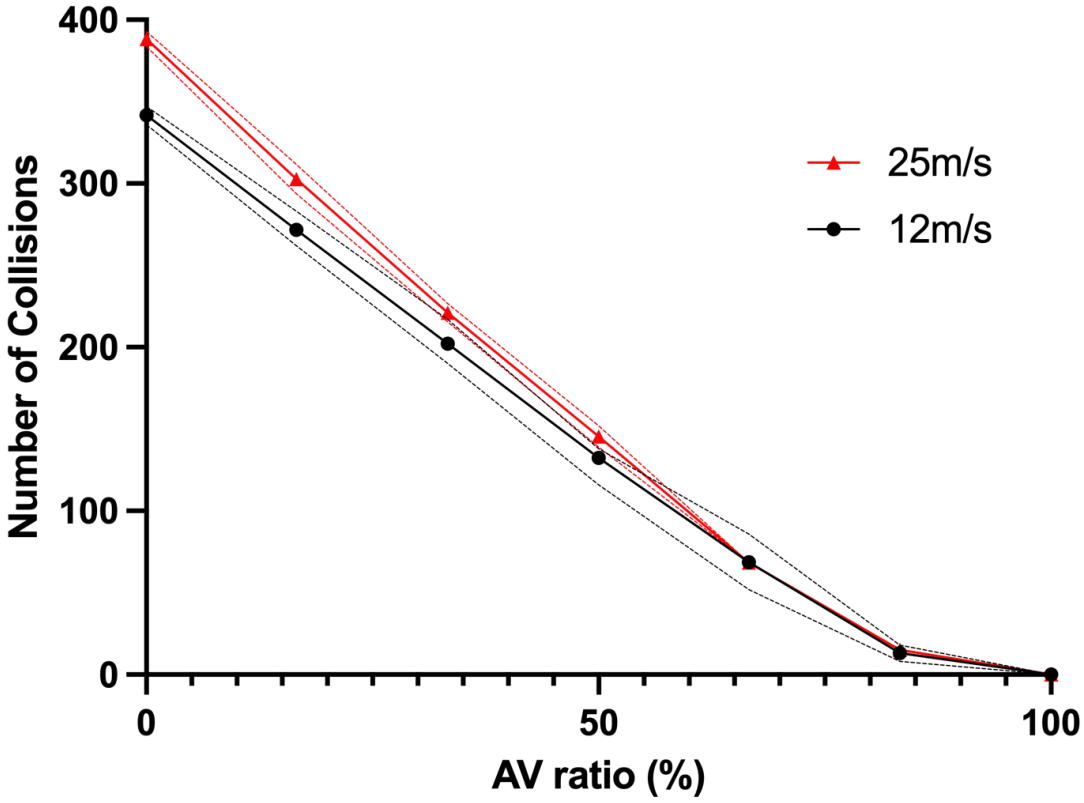

Figure 6.2: The number of collisions by AV ratio.

6.1 Safety Evaluation

To evaluate the safety of **BlaFT**, we checked the number of collisions as AV-ratio differs. Whenever vehicles engaged in accident, they are teleported automatically to different random points on the track by SUMO so that they can continue driving from there. Therefore there at always 30 vehicles present in the simulation.

As shown in Fig. 6.2, the result tells that the number of collisions decreased linearly, as ratio of the number of BlaFT versus the number of human-driven vehicles increased. When the ratio became 100%, the number of collision reduced to zero. And this was common in both of the velocities ($12m/s$, $25m/s$). The linear decrease of the number of collisions came from the fact that each **BlaFT** maintains the response distance and reacts properly to the sudden danger. Interestingly, the safety does not

significantly depend on the required deceleration rate or the length of RE of **BlaFT**.

6.2 Efficiency Evaluation

The efficiency is evaluated by the average delay time as AV-ratio differs. And it is depicted in a Fig. 6.3. First, as **BlaFT** ratio increased, the average delayed time decreased with both of the maximum velocities. This is due to the safe driving of **BlaFT**, since it reduces the accidents which cause the multiple vehicles' delayed time to increase.

Furthermore, when it comes to the slower traffic where the maximum velocity is $12m/s$, it shows that there was no significant impact of the required braking rate or the length of RE on the average delay. However, in the faster traffic where its maximum velocity is 25m/s, it resulted in the larger delayed times compared to the slower traffic. Also, when the response deceleration rate was at a minimum ($2.0m/s^2$), the delay did not change significantly compared to HV-only traffic. However, with other response deceleration rates ($4.5m/s^2$, $7.0m/s^2$), they showed 25% and 34% decrease in delayed time.

This is because the key factor that affects the delayed time is the 'length of RE.' First, in the slow traffic, **BlaFT** maintains the shorter RE compared to the ones in the fast traffic. However, as the traffic gets faster and the area of RE gets wider. At last, **BlaFT** has more chances of RE overlap and this leads to the frequent braking. However, BlaFT can reduce the length of RE by increasing the response deceleration rate up to maximum deceleration rate. Then, **BlaFT** is able to maintain shorter RE even in the faster traffic. In fact, the whole traffic has more chances of being efficient, if BlaFT endures the rapid braking to avoid the collision area and thus maintains shorter RE.

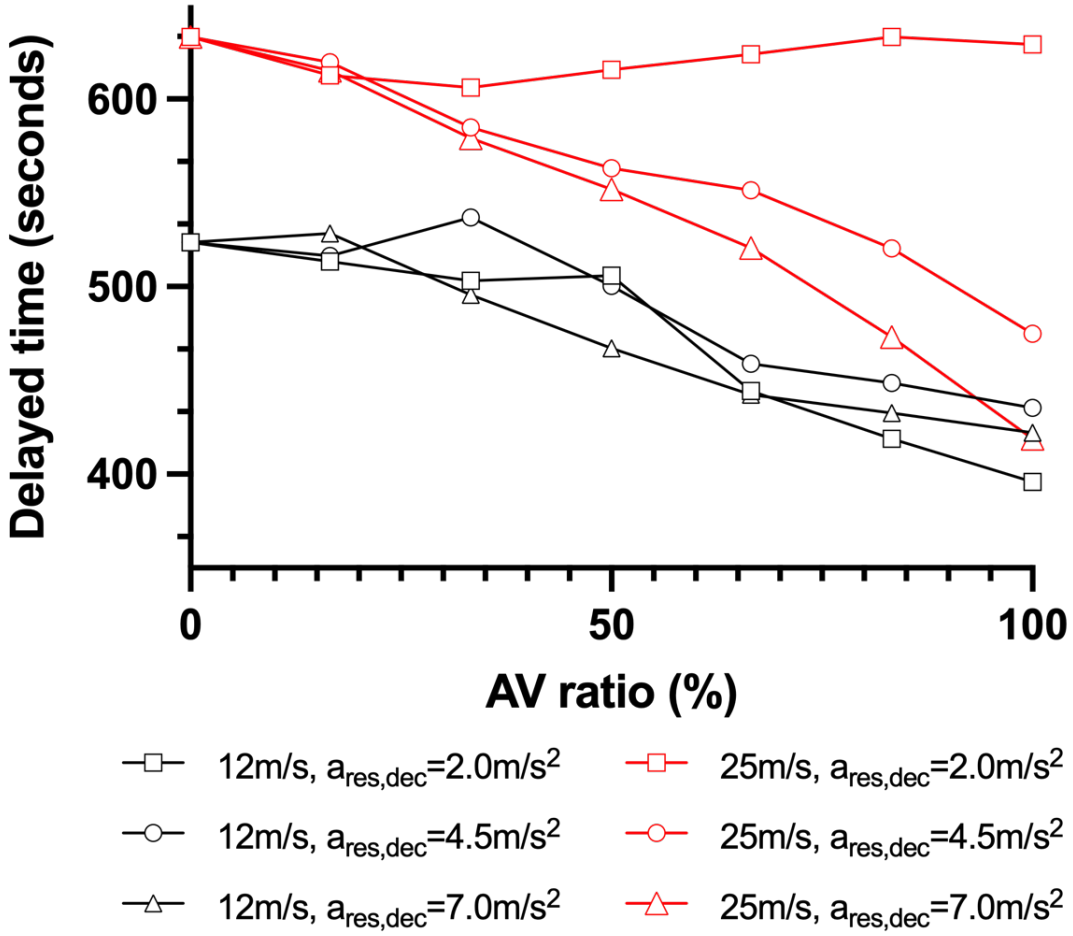

Figure 6.3: Average delayed time by AV ratio.

CONCLUSION

In this paper we proposed '**Bla**me-**F**ree motion planner for hybrid **T**raffic (**BlaFT**)', a motion planner for AVs operating in a hybrid traffic environment with human drivers. We prove both mathematically and empirically via simulation that and AV using BlaFT will neither be the cause of an accident or be blamed for an accident that does involve it. Additionally we have provided a set of equations that can be used to apply blame in the case that there is a crash and sensor data available. In the future we would like to further explore parameters of BlaFT such as the Response Envelope deceleration rate as well as other heuristics for choosing a more optimal path that still conforms to the safety and blame constraints, but will be less likely to cause traffic delays.

REFERENCES

[1] Martin Hilscher, Sven Linker, Ernst-Rüdiger Olderog, and Anders P Ravn. An abstract model for proving safety of multi-lane traffic manoeuvres. In International Conference on Formal Engineering Methods, pages 404–419. Springer, 2011.

[2] Shai Shalev-Shwartz, Shaked Shammah, and Amnon Shashua. On a formal model of safe and scalable self-driving cars. arXiv preprint arXiv:1708.06374, 2017.

[3] Steven Loveday. Mercedes to accept liability when autonomous drive pilot is engaged. International journal of automotive technology, 2022.

[4] Marcel Kahan. Causation and incentives to take care under the negligence rule. The Journal of Legal Studies, 18(2):427–447, 1989.

[5] Pablo Alvarez Lopez, Michael Behrisch, Laura Bieker-Walz, Jakob Erdmann, Yun-Pang Flötteröd, Robert Hilbrich, Leonhard Lücken, Johannes Rummel, Peter Wagner, and Evamarie Wießner. Microscopic traffic simulation using sumo. In The 21st IEEE International Conference on Intelligent Transportation Systems. IEEE, 2018.

[6] Roald J Van Loon and Marieke H Martens. Automated driving and its effect on the safety ecosystem: How do compatibility issues affect the transition period? Procedia Manufacturing, 3:3280–3285, 2015.

[7] Sven Nyholm and Jilles Smids. Automated cars meet human drivers: responsible human-robot coordination and the ethics of mixed traffic. Ethics and Information Technology, 22(4):335–344, 2020.

[8] Hongtao Yu, H Eric Tseng, and Reza Langari. A human-like game theory-based controller for automatic lane changing. Transportation Research Part C: Emerging Technologies, 88:140–158, 2018.

[9] C Fox, F Camara, G Markkula, R Romano, R Madigan, N Merat, et al. When should the chicken cross the road? Game theory for autonomous vehicle-human interactions, 2018.

[10] Andreas Tamke, Thao Dang, and Gabi Breuel. A flexible method for criticality assessment in driver assistance systems. In 2011 IEEE Intelligent Vehicles Symposium (IV), pages 697–702. IEEE, 2011.

[11] Janghee Park, Dongchan Kim, and Kunsoo Huh. Emergency collision avoidance by steering in critical situations. International journal of automotive technology, 22(1):173–184, 2021.

[12] Ishan Tyagi. Threat assessment for avoiding collsions with perpendicular vehicles at intersections. In 2021 IEEE International Conference on Electro Information Technology (EIT), pages 184–187. IEEE, 2021.

[13] Ivó Coca-Vila. Self-driving cars in dilemmatic situations: An approach based on the theory of justification in criminal law. Criminal Law and Philosophy, 12(1):59–82, 2018.

[14] Robin Schubert, Eric Richter, and Gerd Wanielik. Comparison and evaluation of advanced motion models for vehicle tracking. In 2008 11th international conference on information fusion, pages 1–6. IEEE, 2008.

[15] Jeffrey Wishart, Steven Como, Maria Elli, Brendan Russo, Jack Weast, Niraj Altekar, Emmanuel James, and Yan Chen. Driving safety performance assessment metrics for ads-equipped vehicles. SAE Technical Paper, 2(2020-01-1206), 2020.